

Retardation and reduction of pulse distortion by group-velocity dispersion through pulse shaping

Danny Eliyahu, Randal A. Salvatore, Joseph Rosen, Amnon Yariv, and Jean-Jacques Drolet

California Institute of Technology, M/S 128-95, Pasadena, California 91125

Received February 15, 1995

We show that a reduction in the pulse distortion caused by chromatic dispersion can be achieved through pulse shaping. We argue that a simple binary phase mask in the Fourier plane of the laser spectrum can improve the transmission of short pulses in a dispersive channel through reduced broadening. The argument was tested experimentally, and a good agreement was found with the theory.

Optically transmitted pulses in a single-mode channel can be severely distorted and broadened as the result of chromatic dispersion. Several methods have been used to overcome the distortion of the pulse envelope caused by group-velocity dispersion (GVD): a grating pair,¹ a Fabry-Perot interferometer,² a phase conjugator,³ a laser modulated with a periodic injection current sweep,^{4,5} and time lenses for Gaussian-shaped pulses.⁶ In soliton propagation self-phase modulation compensates the GVD of a hyperbolic secant pulse shape.⁷

With z denoted as the position along the dispersive channel, v_g as the group velocity, and $T = t - z/v_g$ as the delayed time, the influence of GVD on the complex temporal pulse electric field $u(T, z)$ envelope is given by⁸

$$u(T, z) = \int_{-\Delta\omega/2}^{\Delta\omega/2} U(\omega, z=0) \exp\left(\frac{i\beta_2 z \omega^2}{2} - i\omega T\right) d\omega, \quad (1)$$

where $U(\omega, 0)$ is the Fourier transform of $u(T, 0)$, ω is the angular frequency (relative to the laser's center frequency ω_0), $\Delta\omega$ is the spectral width corresponding to the pulse, and $\beta_2 = \partial^2 \beta / \partial \omega^2|_{\omega_0}$ is the GVD per unit length.

Recently^{9,10} the possibility of pulses that do not disperse by virtue of their unique shaping was introduced. Based on the time-space analogy Rosen *et al.*⁹ proposed

$$u(T, 0) = u_C(T, 0) = \frac{1}{\sqrt{2i\pi\beta_2 f}} \int_{-\infty}^{\infty} \cos\left[\left|\frac{t'}{b}\right|^p - \left(\frac{t'}{a}\right)^2\right] \times \exp\left(i\frac{Tt'}{\beta_2 f}\right) dt' \quad (2)$$

as the initial pulse envelope to reduce the effect of GVD. a, b, f , and $p > 2$ are real positive parameters of the pulse. This pulse ($u = u_C$, $\Delta\omega = \infty$) propagates along a dispersive channel at a distance of $\Delta z \approx 2\sqrt{2\pi}\beta_2 f^2 p[4(1+p)]^{(2-p)/p}/b^2$ while maintaining a near-constant peak value of $|u_C(0, z)|$.

The spectrum of u_C is

$$U(\omega, 0) = U_C(\omega, 0) = \cos[(T_b \omega)^4 - (T_a \omega)^2], \quad (3)$$

where $T_b = \beta_2 f / b$, $T_a = \beta_2 f / a$, and the power $p = 4$ has been chosen as an example.

In what follows we describe an experimental investigation of the possibility of creating dispersion-resistant pulses through pulse shaping and show that it can be accomplished by use of a simple binary phase mask in the spectral plane. We find that using a binary approximation of the initial pulse spectrum [Eq. (3)], $U_B(\omega, 0) = U_C(\omega, 0)/|U_C(\omega, 0)|$, still leads to a considerable reduction in pulse distortion. This approximation enables us to use a binary (0 or π) phase mask instead of a complicated amplitude and phase filter.

The pulse field U_B and its capability of maintaining its form without distortion when traveling through a dispersive channel depend on the ratio T_b/T_a . We find numerically that $T_b/T_a = \sqrt{8/5}$ is sufficient in that the intensity $I_B(T = 0, z) = |u_B(0, z)|^2$ of the center of the symmetric pulse and its shape remains at a nearly constant height over the interval $\Delta z \approx 8T_b^2/\beta_2$ near $z = 0$. One may increase this interval by increasing the ratio T_b/T_a , yet increasing the interval spoils the constancy of $I_B(0, z)$ in the region of interest. At $z = 0$ the pulse has a main lobe width around $T = 0$ of order T_b and a tail length that depends on $T_b \Delta\omega$. Although reducing $T_b \Delta\omega$ reduces the pulse tail length, it increases the tail intensity compared with $I_B(0, 0)$ and introduces small oscillations in $I_B(0, z)$ as a function of z .

In Fig. 1 the pulse intensity shape $I(T, z)$ normalized by $I(0, 0)$ is shown as a function of the delayed time T for different values of GVD, i.e., the normalized distance $\beta_2 z / 2T_b^2$. Figures 1(a)–1(d) describe $I_B(T, z)/I_B(0, 0)$ with a binary phase mask, $U(\omega, 0) = U_B(\omega, 0)$ and $T_b \Delta\omega = 4.044$, using the first nine lobes of the cosine spectrum function of Eq. (3). The pulse maintains its basic form and height even for $\beta_2 z / 2T_b^2 = 1.6$, as can be seen from comparison among Figs. 1(a)–1(c). In these cases the main lobe of the pulse envelope as well as $I_B(0, z)$ is essentially invariant. The changes that are due to chromatic dispersion are mostly in the tails. The reduction of $I_B(0, z)$ for $\beta_2 z / 2T_b^2 = 0.8$ [Fig. 1(b)] is a result of finite $T_b \Delta\omega$, as mentioned above. Note that this result is independent of the sign of β_2 because $I_B(0, -z) = I_B(0, z)$. Therefore, in practice one can exploit this fact and shape the pulse $u_B(T, \sim -4T_b^2/\beta_2)$ at the beginning of the dispersive channel and use the full interval of $8T_b^2/\beta_2$.

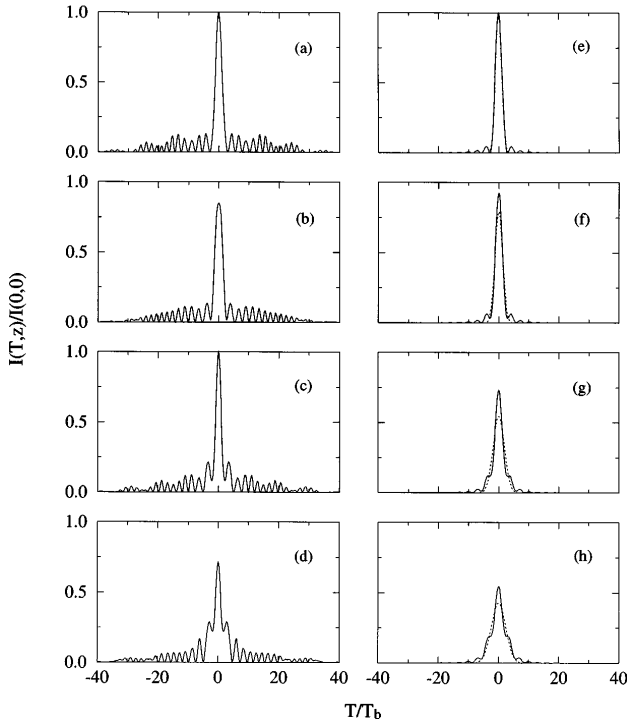


Fig. 1. Pulse intensity $I(T, z)$ normalized by $I(0, 0)$ versus T/T_b for different values of $\beta_2 z / 2T_b^2$. (a)–(d) $U(\omega, 0) = U_B(\omega, 0)$ and $T_b \Delta\omega = 4.044$. (e)–(h) The solid curves result from $U_S(\omega, 0) = 1$ and $T_b \Delta\omega = 2.156$ having the same pulse main lobe width at $z = 0$; the dotted curves represent a Gaussian pulse with the same pulse width at $z = 0$. The GVD is equal to zero in (a) and (e), whereas for (b) and (f) $\beta_2 z / 2T_b^2 = 0.8$, for (c) and (g) $\beta_2 z / 2T_b^2 = 1.6$, and for (d) and (h) $\beta_2 z / 2T_b^2 = 2.2$.

These results are compared with those from a rectangular spectrum without the phase mask. For this comparison [the solid curves in Figs. 1(e)–1(h)] we choose $U(\omega, 0) = U_S(\omega, 0) = 1$ and spectral width $\Delta\omega_s = 2.156/T_b$ to generate the same pulse main lobe width as with the mask. The pulse shape is $I_S(T, 0)/I_S(0, 0) = \text{sinc}^2(\Delta\omega_s T)$, where $\text{sinc}(x) = \sin(x)/x$. The primary difference between the pulse's U_B [Eq. (2)] and U_S is in the tails. The second pulse has shorter tails and therefore suffers more distortion and reduction of $I(0, z)$ compared with $I(0, 0)$ along its propagation in the dispersive channel.

Results for the familiar Gaussian pulse [the dotted curves in Figs. 1(e)–1(h)] are also compared. This pulse has just one lobe and suffers a reduction of $I_G(0, z)$ even at distances shorter than those of U_S . Its complete dependence on T and z can be written in closed form and is given by

$$\frac{I_G(T, z)}{I_G(0, 0)} = \frac{\exp\left\{-\frac{T^2}{T_G^2[1 + (\beta_2 z / T_G^2)^2]}\right\}}{[1 + (\beta_2 z / T_G^2)^2]^{1/2}}. \quad (4)$$

We chose $T_G = 1.44T_b$ so that the main lobe width is identical to that of the two cases described above at $z = 0$. From Figs. 1(c) and 1(g) one can see that although the Gaussian pulse decays to 54% of its initial intensity [Fig. 1(g)], the pulse with the U_B spectrum maintains its value.

The above theoretical results were tested experimentally for the cases of U_B and the rectangular spectrum U_S . The experimental setup is shown in Fig. 2. The laser is a passively mode-locked quadruple quantum-well two-section, GaAs buried heterostructure as described previously.^{11,12} Its spectrum is between 839.9 and 845.2 nm. The pulse spectrum is approximated by a rectangular function with a quadratic phase.^{11,12} The laser pulses were sent to a telescoped dual-grating compressor ($1/d = 2000$ lines/mm) to achieve pulse shaping,¹³ laser chirp cancellation, and GVD addition. Different optical frequency components of the input laser pulse are spatially dispersed by the grating at the left and then resolved spatially in the Fourier plane of the lens. At this plane the spectrum is filtered through either the spatial binary phase mask or a window to reshape the pulse. The spectrum is recombined spatially by a second lens and grating. We easily achieve laser chirp cancellation and GVD addition by moving the grating at the right in Fig. 2. We cancel the laser chirp by simply moving the grating to minimize the pulse width (without the phase mask or the window) and specifying the position of the grating as $z = 0$. Then the phase mask is introduced in the Fourier plane and autocorrelation measurements are taken for different positions z of the right-hand grating. The GVD is given by¹⁴

$$\frac{\beta_2 z}{2T_b^2} = \frac{\lambda_0^3 z}{4\pi T_b^2 c^2 d^2 \cos^2(\theta)}, \quad (5)$$

where z is the distance of the right-hand grating location along the central axis of the dual-grating compression system. Also, $\theta = 51.1^\circ$ is the angle between this axis and the normal to the grating surface, $\lambda_0 = 2\pi c/\omega_0$ is the optical carrier wavelength, and c is the velocity of light.

The reshaped pulses are sent into a Michelson interferometer and a second-harmonic generation crystal to measure their temporal autocorrelation. Autocorrelations were taken for the case when $U(\omega, 0) = U_B(\omega, 0)$ and $T_b \Delta\omega = 4.044$. We find numerically that the pulse shape is insensitive to small variations in the amplitude distribution of the spectrum. Therefore the assumption of a rectangular function between $-\Delta\omega/2$ and $\Delta\omega/2$ for the laser amplitude spectrum is justified, and the need for

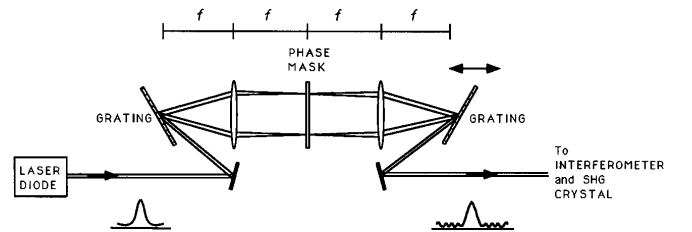


Fig. 2. Fourier-transform pulse shaping, compression, and fiber GVD simulated apparatus. Optical frequency components of the input laser pulse are spatially dispersed and filtered through the spatial binary phase mask to reshape the pulse and then spatially recombined. The left-hand grating is placed in the focal point of the lens, whereas the right-hand grating is movable to achieve compression and different chirp values for GVD.

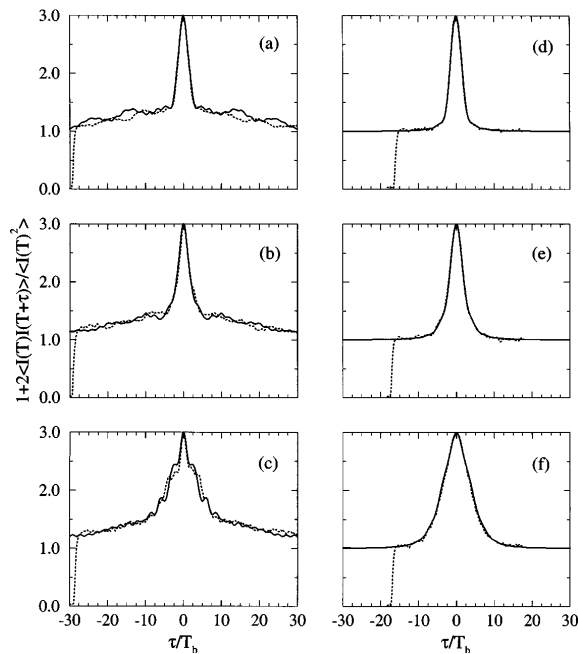


Fig. 3. Comparison between experimental (dotted curves) and theoretical (solid curves) autocorrelation results. (a)–(c) $U(\omega, 0) = U_B(\omega, 0)$ and $T_b \Delta\omega = 4.044$; (d)–(f) $U_S(\omega, 0) = 1$ and $T_b \Delta\omega = 2.156$. The measurements were taken for different GVD's: (a), (d) $\beta_2 z / 2T_b^2 = 0$; (b), (e) $\beta_2 z / 2T_b^2 = 1.1$; (c), (f) $\beta_2 z / 2T_b^2 = 2.2$.

a complicated mask is reduced to that for a simple binary phase mask. The mask, made by photolithography,¹⁵ has a width of 3.4 mm (the spatial width of the optical spectrum in the Fourier plane), which is equivalent to $\Delta\omega = 13.3 \times 10^{12}$ rad/s. The mask was encircled by a window of the same width to eliminate undesirable influences from the tails of the spectrum. The index of refraction of the glass mask is $n = 1.5$; therefore the depth of the etching is λ_0 . The autocorrelations measured while the phase mask is used are given in Figs. 3(a)–3(c). Two parameters (T_b and β_2) describe the fit between the theoretical (solid curves) and experimental (dotted curves) autocorrelation results. First, for $z = 0$ [Fig. 3(a)] the parameter T_b was found to be equal to $T_b = 370$ fs, whereas the theoretical calculation gives $T_b = 4.044/\Delta\omega \approx 340$ fs). A second measurement [Fig. 3(b)] was taken at $\beta_2 z / 2T_b^2 = 1.1$ ($z = 2.5$ cm) to specify the second parameter β_2 (theoretical calculation gives $\beta_2 z / 2T_b^2 = 1.16$ at this location). A third measurement [Fig. 3(c)] was taken for $\beta_2 z / 2T_b^2 = 2.2$. A good fit is indicated between theory and experimental results.

A similar series of autocorrelations was measured without the phase mask, in which $U_S(\omega, 0) = 1$ and $T_b \Delta\omega = 2.156$, to check the rectangular spectrum case. In this case a window was located in the Fourier plane, allowing the center of the laser spectrum to pass and blocking the rest of the spectrum. Its width was adjusted to give the same autocorrelation half-width, which is nearly equivalent to getting the same main lobe pulse width as with the phase mask. The allowed spectrum had $\Delta\omega \approx 6.62 \times 10^{12}$ rad/s. The results of

this experiment are shown in Figs. 3(d)–3(f). The fit was done without any free parameters. The same values of T_b and $\beta_2 z / 2T_b^2$ as before were used. A good agreement between theory and the experimental results was found again.

Two differences are prominent from the different pulses used to generate Figs. 3(a)–3(f). First, the autocorrelation tails in Figs. 3(a)–3(c) for the pseudo-nondispersive pulse (U_B) decay slowly, reaching the background value of 1 only for very large τ . This is a direct result of the pulse tail, as can be seen from Figs. 1(a)–1(d). The U_S pulse, which has a much shorter tail, has autocorrelations that reach the value of 1 [Figs. 3(d)–3(f)] for smaller τ . Second, for higher values of $\beta_2 z / 2T_b^2$ the autocorrelation has the form of a cascade. This occurs when the main lobe of the pulse [Fig. 1(d)] becomes comparable in magnitude with the secondary lobes on each side. The width of the autocorrelation for small τ/T_b indicates the width of the main peak of the pulse.

In conclusion, the possibility of pulse shaping to reduce the distortion caused by GVD was theoretically considered and checked experimentally. It was found that a simple phase mask in the spectral plane can add tails with many lobes, which considerably alleviate distortion to the main lobe of the pulse for longer propagation distances in dispersive channels than for other pulses.

This research was supported by the National Science Foundation and the Advanced Research Projects Agency.

References

- O. E. Martinez, IEEE J. Quantum Electron. **23**, 59 (1987).
- L. J. Cimini, L. J. Greenstein, and A. A. M. Sleh, J. Lightwave Technol. **8**, 649 (1990).
- A. Yariv, D. Fekete, and D. Pepper, Opt. Lett. **4**, 52 (1979).
- N. Henmi, T. Saito, and T. Ishida, J. Lightwave Technol. **12**, 1706 (1994).
- T. L. Koch and R. C. Alferness, J. Lightwave Technol. **LT-3**, 800 (1985).
- S. P. Djaili, A. Dienes, and J. S. Smith, IEEE J. Quantum Electron. **QE-6**, 1158 (1990).
- L. F. Mollenauer and K. Smith, Opt. Lett. **13**, 675 (1988).
- A. Yariv, *Optical Electronics*, 4th ed. (Saunders, Philadelphia, Pa., 1991), p. 62.
- J. Rosen, B. Salik, A. Yariv, and H. K. Liu, Opt. Lett. **20**, 423 (1995).
- B. Salik, J. Rosen, and A. Yariv, "One-dimensional beam shaping," J. Opt. Soc. Am. A (to be published).
- R. A. Salvatore, T. Schrans, and A. Yariv, Opt. Lett. **20**, 737 (1995).
- S. Sanders, A. Yariv, J. Paslaski, J. E. Ungar, and H. A. Zarem, Appl. Phys. Lett. **58**, 681 (1991).
- A. M. Weiner, J. P. Heritage, and E. M. Kirschner, J. Opt. Soc. Am. B **5**, 1563 (1988).
- E. B. Treacy, IEEE J. Quantum Electron. **QE-5**, 454 (1969).
- D. C. O'Shea, J. W. Beletic, and M. Poutous, Appl. Opt. **32**, 2566 (1993).